A bound on Ekman pumping

Stephan R. de Roode[1]*, A. Pier Siebesma[12],

[1]Delft University of Technology, The Netherlands.
[2]KNMI, De Bilt, The Netherlands.

Key Points:

- The large-scale vertical velocity caused by boundary-layer turbulent friction has a maximum value.

*Department of Geosciences and Remote Sensing, Faculty of Civil Engineering and Geosciences, Delft University of Technology, Stevinweg 1, 2628 CN Delft, The Netherlands

Corresponding author: S. R. de Roode, s.r.deroode@tudelft.nl

Abstract

Momentum transport by boundary-layer turbulence causes a weak synoptic-scale vertical motion. The classical textbook solution for the strength of this Ekman pumping depends on the curl of the surface momentum flux. In this study a new solution for Ekman pumping for low Rossby number flow is derived. In particular, the surface momentum flux is parameterized with a commonly used bulk drag formula. This step reveals that the strength of Ekman pumping is bounded. A maximum value is found if the angle between the near-surface wind and the geostrophic wind is 45°. The weakening of Ekman pumping for enhanced turbulent friction can be simply explained from the fact that an enhanced turbulent drag will reduce the horizontal wind. This may eventually diminish its capacity for large-scale convergence of divergence. As momentum transport is parameterized in large-scale models, the analysis is relevant for the understanding and interpretation of the evolution of synoptic-scale vertical motions as predicted by such models.

1 Introduction

Geostrophic flow is at the heart of dynamical meteorology. It elucidates why in a synoptic system of (low) high pressure on the northern hemisphere the wind vector is tangent to the isobars in a (counter-)clockwise direction. However, this theoretical wind structure is fully two-dimensional with a zero vertical velocity component. In fact, the presence of synoptic-scale vertical motion actually requires the consideration of turbulent boundary-layer eddies that act as a drag on the mean flow. As depicted schematically in Fig. 1, this friction effect gives rise to a net horizontal transport of air from high to low pressure. The resulting accumulation of mass drives a large-scale upwards vertical velocity in a low pressure system, and vice versa in a high pressure system. Because the magnitude of the turbulent friction controls the strength of the cross-isobaric flow [*Svensson and Holtslag*, 2009], it impacts the evolution of (anti) cyclones at synoptic scales [*Sandu et al.*, 2013].

Although the characteristic synoptical-scale vertical velocity is small, typically on the order of $\mathrm{cm\,s^{-1}}$, its effect on the evolution of the boundary layer cannot be neglected. For example, large-scale subsidence tends to advect the boundary-layer top downwards

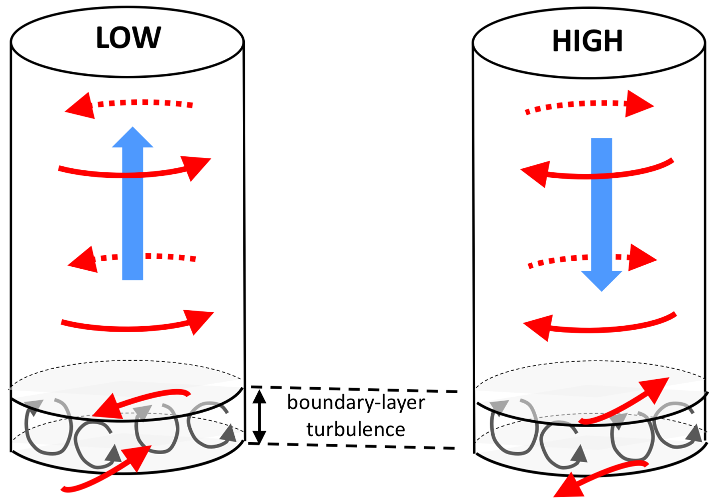

Figure 1. A schematic representation of Ekman pumping in a synoptic low and high pressure system (adapted from *Marshall and Plumb* [2016]).

[*Lilly*, 1968], which has a strong impact on the concentration of air pollution in the atmospheric boundary layer [*Seibert et al.*, 2000], the evolution of subtropical stratocumulus [*Zhang et al.*, 2009; *Van der Dussen et al.*, 2016], and Arctic mixed-phase stratocumulus [*Young et al.*, 2018].

Various efforts have been made to assess the large-scale subsidence from field observations of horizontal wind and with use of the equation for conservation of mass,

$$\frac{\partial U}{\partial x} + \frac{\partial V}{\partial y} + \frac{\partial W}{\partial z} = 0, \tag{1}$$

with U, V, W the east-west (x), north-south (y) and vertical (z) components of the wind vector, respectively. The mean vertical velocity is controlled by the large-scale divergence of horizontal wind,

$$D \equiv \left(\frac{\partial U}{\partial x} + \frac{\partial V}{\partial y}\right) = -\frac{\partial W}{\partial z}. \tag{2}$$

This diagnostic expression proved useful to study the diurnal cycle of D from radiosondes that were launched during the Atlantic Stratocumulus Transition Experiment [*Ciesielski et al.*, 1999]. *Lenschow et al.* [2007] studied aircraft measurements of the horizontal wind field collected from circular legs flown during the Second Dynamics and Chemistry of Marine Stratocumulus (DYCOMS-II) experiment and concluded that this measurement strategy is not suitable to diagnose D as it yields unacceptable large errors. By contrast, *Bony et al.* [2017] demonstrated that the use of dropsondes rather than direct aircraft observations of horizontal wind can actually be rather well used to determine D with a sufficient accuracy.

A well known and frequently used solution for the mean vertical motion depends on the curl of the surface momentum flux [*Beare*, 2007]. In this note a new diagnostic equation for the large-scale divergence of the horizontal wind D in terms of the strength of a non-dimensional turbulent boundary-layer friction factor will be derived. It will be demonstrated that this solution predicts a maximum value for the large-scale divergence of the horizontal wind.

2 Theory

The dependency of the large-scale vertical velocity on the horizontal structure of the surface momentum flux can be readily obtained from the conservation equations for momentum and mass. Here we will extend this derivation by applying a bulk parameterization for the surface momentum flux.

2.1 Governing equations

The horizontal momentum equations read,

$$\frac{dU}{dt} = fV - \frac{1}{\rho}\frac{\partial P}{\partial x} - \frac{\partial \overline{uw}}{\partial z}, \tag{3}$$

$$\frac{dV}{dt} = -fU - \frac{1}{\rho}\frac{\partial P}{\partial y} - \frac{\partial \overline{vw}}{\partial z}, \tag{4}$$

with P the pressure, f the Coriolis parameter, and $\overline{uw}$ and $\overline{vw}$ the Reynolds averaged momentum fluxes. The main goal of this note is to study the effect of boundary-layer friction. So baroclinic effects will be ignored and consequently a constant density ρ will be used. We will also limit ourselves to large-scale motions with small Rossby number values. This allows to neglect the total derivative of the wind by approximating it to zero. We refer the interested reader to the studies by *Wu and Blumen* [1982] and *Tan* [2001] that report on effects of non-linear advection and baroclinicity, respectively, on the large-scale vertical velocity in atmospheric boundary-layers.

In the absence of turbulence a geostrophic balance is maintained by the Coriolis and the pressure gradient forces,

$$U = U_{\mathrm{g}} \equiv -\frac{1}{\rho f}\frac{\partial P}{\partial y} \quad , \quad V = V_{\mathrm{g}} \equiv \frac{1}{\rho f}\frac{\partial P}{\partial x}, \tag{5}$$

with U_g and V_g defining the geostrophic wind velocity components. A substitution of these solutions in Eq. (2) gives $D = 0$, such that a pure geostrophic flow does not support any mean vertical motion.

The importance of turbulence on the vertical motion becomes clear after a differentiation of Eqs. (3) and (4) with respect to y and x, respectively, and the use of these expressions in Eq. (2),

$$\beta V - \frac{\partial}{\partial z}\left[fW - \frac{\partial \overline{uw}}{\partial y} + \frac{\partial \overline{vw}}{\partial x}\right] = 0. \tag{6}$$

Here we reversed the order of differentiation in the pressure and momentum flux terms. The latitudinal variation of the Coriolis parameter f is quantified by the parameter $\beta = df/dy$. An estimation of the magnitude of this term can be made by considering a latitude of 30° on the Northern hemisphere where $\beta = 1.6 \times 10^{-11}\mathrm{m}^{-1}\mathrm{s}^{-1}$. In the Hadley cell over the subtropical oceans $V \sim -10\mathrm{ms}^{-1}$ (in the southward direction), which leaves $\partial W/\partial z = \beta V/f \sim -1.6 \times 10^{-6}\mathrm{s}^{-1}$. Although this is not an insignificant contribution to the large-scale subsidence typically observed in this region, in the remainder we will ignore the latitudinal variation of the Coriolis parameter f by setting the factor $\beta = df/dy$ to zero. The vertical gradient of W has entered equation (6) by the use of the continuity equation (1). A vertical integration from the surface (indicated by the subscript 'sfc') upwards to the height h^+, which is just above the boundary layer where turbulence vanishes, shows that the vertical velocity depends on the curl of the surface momentum fluxes [*Beare*, 2007],

$$W|_{h^+} = \frac{1}{f}\left(\frac{\partial \overline{uw}_{\mathrm{sfc}}}{\partial y} - \frac{\partial \overline{vw}_{\mathrm{sfc}}}{\partial x}\right), \tag{7}$$

with $W = 0$ at the ground surface. The vertical velocity that is driven by surface momentum fluxes is called Ekman pumping after the Swedish oceanographer who was the first to derive an analytical solution for wind-driven horizontal transport in the ocean. Ekman's solution for ocean flow is widely used as a powerful diagnostic tool that relates the strength of Ekman pumping in the ocean to the curl of the wind stress exerted at the Ocean's surface.

2.2 Parameterization of the momentum flux

The surface momentum fluxes can be expressed by the following bulk formula,

$$(\overline{uw}_{\mathrm{sfc}}, \overline{vw}_{\mathrm{sfc}}) = -C_{\mathrm{d}} U_{\mathrm{s}} (U, V), \tag{8}$$

with

$$U_\mathrm{s} = \sqrt{U^2 + V^2}. \tag{9}$$

The factor C_d is turbulent drag coefficient that depends on the vertical stability and the roughness length [*Schröter et al.*, 2013]. The stationary momentum equations can then be expressed as follows,

$$f(V - V_\mathrm{g}) - \frac{C_\mathrm{d} U_\mathrm{s}}{h} U = 0, \quad , \quad -f(U - U_\mathrm{g}) - \frac{C_\mathrm{d} U_\mathrm{s}}{h} V = 0. \tag{10}$$

Because of the presence of U_s this is a non-linear set of equations.

Marshall and Plumb [2016] further simplify the effect of the surface momentum fluxes by introducing a bulk surface drag factor

$$k_\mathrm{sfc} = C_\mathrm{d} U_\mathrm{s}. \tag{11}$$

If there is no entrainment of momentum at the top of the boundary layer, which implies that the momentum flux at height h is assumed to be zero, then the bulk effect of the momentum fluxes can be expressed as

$$\frac{\partial}{\partial z}(\overline{uw}, \overline{vw}) = \frac{k_\mathrm{sfc}}{h}(U, V). \tag{12}$$

With aid of the parameterization we can write the stationary momentum equations as follows,

$$V - V_\mathrm{g} - k_\mathrm{f} U = 0, \quad , \quad -U + U_\mathrm{g} - k_\mathrm{f} V = 0. \tag{13}$$

Here we introduced a non-dimensional factor k_f,

$$k_\mathrm{f} = \frac{C_\mathrm{d} U_\mathrm{s}}{f h}, \tag{14}$$

which can be interpreted as a turbulent Ekman number as it compares the importance of the accelerations due to the turbulent ("viscous") drag and the Coriolis force.

To provide insight in the dependency of the horizontal wind on the non-dimensional turbulent boundary-layer friction we will discuss the analytical solution of (13) in the next section.

3 Analytical solution for the large-scale subsidence

Here we present and discuss the analytical solutions for the large-scale flow that follows from the steady-state linearized momentum equations (13).

3.1 Steady-state analytical solutions

The solutions for the horizontal wind can be expressed in terms of the geostrophic wind,

$$U = \frac{U_\mathrm{g} - k_\mathrm{f} V_\mathrm{g}}{1 + k_\mathrm{f}^2} \quad , \quad V = \frac{V_\mathrm{g} + k_\mathrm{f} U_\mathrm{g}}{1 + k_\mathrm{f}^2}. \tag{15}$$

With aid of Eq. (2) it is found that the large-scale divergence of the horizontal wind field depends on both the curl of the geostrophic wind,

$$D = F(k_\mathrm{f}) \left(\frac{\partial U_\mathrm{g}}{\partial y} - \frac{\partial V_\mathrm{g}}{\partial x} \right), \tag{16}$$

where we introduced the function

$$F(k_\mathrm{f}) = \frac{k_\mathrm{f}}{1 + k_\mathrm{f}^2}. \tag{17}$$

We note that by using the solution of geostrophic equilibrium Eq. (5) we can express D as a Poisson equation,

$$D = -\frac{F(k_\mathrm{f})}{\rho f} \nabla^2 P. \tag{18}$$

The function F is also present in the solution for the large-scale vertical velocity, which magnitude at the top of the boundary layer can be readily obtained from a vertical integration of D,

$$w|_h = -F(k_\mathrm{f}) \left(\frac{\partial U_\mathrm{g}}{\partial y} - \frac{\partial V_\mathrm{g}}{\partial x} \right) h, \tag{19}$$

where we tacitly assumed that the value of D based on the near-surface winds is constant within the boundary layer, which is not an uncommon assumption [*Stevens*, 2006]. However, recent findings based on dropsonde observations suggests that D exhibits quite some variability in the vertical direction [*Bony and Stevens*, 2019].

3.2 Interpretation

Let us first discuss the solutions for the horizontal wind, Eq. (15). In the absence of turbulent friction ($k_\mathrm{f} = 0$) we recover the solutions of geostrophic balance (5). For $k_\mathrm{f} > 0$ the solutions demonstrate that the turbulent boundary-layer friction acts to diminish the wind speed according to

$$U_\mathrm{s} = \sqrt{\frac{U_\mathrm{g}^2 + V_\mathrm{g}^2}{1 + k_\mathrm{f}^2}} \leq |\vec{U}_\mathrm{g}|. \tag{20}$$

As an illustration of the effect of turbulent friction let us consider the simple situation in which the geostrophic forcings $U_\mathrm{g} = 0$ and $V_\mathrm{g} \neq 0$. For frictionless flow $U = 0$. However, for $k_\mathrm{f} > 0$ we find that $U \neq 0$, which indicates that cross-isobaric flow occurs. The presence of this ageostrophic wind component results in the large-scale divergence (or convergence) of the flow that, in turn, drives the large-scale vertical motions.

The solution for the mean vertical velocity (19) is analogous to the one that is expressed in terms of the curl of the surface momentum flux (7). According to Eq. (8) the surface momentum flux depends, to first order, on the mean horizontal wind velocity, which is arguably proportional to the geostrophic wind. However, unlike Eq. (7), the new solution Eq. (19) gives a direct relation between W, the curl of the geostrophic wind, and the non-dimensional turbulent boundary-layer friction factor k_f. We will now argue that k_f puts a bound on the strength of Ekman pumping, a condition that cannot be directly inferred from Eq. (7). To this end let us inspect the function F shown in Fig. 2. For a frictionless purely geostrophic flow the factor $F = 0$, and consequently there will be no large-scale divergence. For the regime $0 \leq k_\mathrm{f} \leq 1$, F increases up to maximum value of 0.5. If the turbulent friction goes to infinity, or equivalently, $k_\mathrm{f} \to \infty$, then $F \to 0$. In this limit turbulent friction damps the horizontal wind to zero, and subsequently the large-scale divergence $D \to 0$. This leads to the key conclusion that the effect of turbulent boundary-layer friction on the large-scale vertical velocity is bounded.

3.3 Discussion

Sandu et al. [2013] evaluated the effect of a less diffusive parameterization for turbulent transport in stably-stratified boundary layers in the European Centre for Medium-Range Weather Forecasts (ECMWF) model, and confirmed that the strength of turbulence diffusion affects the large-scale flow by modulating the strength of synoptic-scale systems. Moreover, they found that the model improved the representation of high-pressure systems, but the storm track region in the Southern Hemisphere was less well captured. Our analysis suggests that the question as to which a change in the parameterization of turbulence in a large-scale weather forecast model leads to either a strengthening or a weakening effect on the evolution of synoptic-scale systems, depends on the value of the factor k_f.

The weakening regime is found for $k_\mathrm{f} > 1$. By setting $U_\mathrm{g} = 0$, it can be easily seen from Eq. (15) that $k_\mathrm{f} = 1$ corresponds to $U = V = \frac{1}{2}V_\mathrm{g}$, which implies that the near surface wind and the geostrophic wind have an angle α of 45°. *Svensson and Holtslag* [2009] investigated results from single column models as obtained from the Global Energy

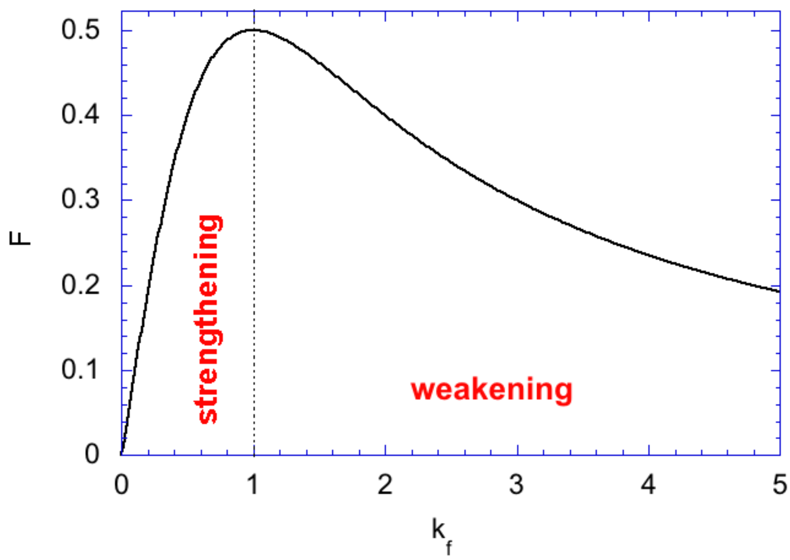

Figure 2. The factor F as a function of k_f as defined by Eq. (17). The vertical dotted line indicates $k_\mathrm{f} = 1$ for which F has its maximum value. The regime $0 < k_\mathrm{f} < 1$ is indicated by 'strengthening', which means that the large-scale divergence D increases for increasing k_f. In the weakening regime, $k_\mathrm{f} > 1$, D will decrease for increasing k_f.

and Water Cycle Experiment (GEWEX) Atmospheric Boundary Layer Study (GABLS1). They found that α varied between 27 and 46° among the models (see their Fig. 6). Since the maximum angle found is slightly beyond the maximum strength for Ekman pumping this finding suggests that our solution of decreasing Ekman pumping under conditions of strong turbulent transport of momentum could be relevant to the understanding and interpretation of model behaviour.

It should be noted that the boundary-layer depth itself is controlled by the strength of turbulence. For example, the enhancement of turbulent diffusion in stable conditions, used to improve the representation of large-scale synoptic systems, leads to an overestimation of the boundary-layer depth [*Sandu et al.*, 2013]. In this case an increase in the surface momentum drag, being proportional to $C_\mathrm{d}U_\mathrm{s}$, is accompanied by an enhanced value of the boundary-layer depth h. Such simultaneous changes could leave the changes in both k_f and F small. For example, in the model intercomparison study by *Svensson and Holtslag* [2009] it was found that the surface momentum fluxes varied by almost a factor of three among the models (see their Fig. 1d). However, because models with higher surface momentum fluxes also had significantly deeper boundary layers, the differences in the vertical gradient of the momentum flux were rather small. Suppose that a change in the turbulent friction is accompanied by a change in the boundary layer depth such that k_f is not affected. According to Eq. (16) D will remain constant (16) for this case, but following Eq. (19) the mean vertical motion at the top will change proportionally to the change of the boundary layer depth.

Observations allow to make some estimations of the magnitude of k_f. Let us consider a situation in the midlatitudes with $f = 10^{-4}$ s^{-1}, and a typical horizontal wind speed $U_\mathrm{s} = 10$ ms^{-1}. Observations collected over the ocean suggest that the order of magnitude for C_d is 0.001 [*Edson et al.*, 2013]. Using Eq. (11) we estimate that for this case F peaks at a boundary layer depth $h = 100$ m. This value for h is rather small, but may be observed under stably stratified surface conditions [*Seidel et al.*, 2010].

Over land the global mean value for the bulk drag coefficient for momentum is approximately one order of magnitude larger as compared to its value over the sea [*Garratt*, 1977]. For land surfaces F therefore exhibits its maximum value for a boundary layer depth h of about 1 km. Such a value of h, but also shallower as well as deeper boundary layers are frequently observed during daytime [*Seidel et al.*, 2012; *von Engeln and Teixeira*, 2013]. Our analysis suggests that for $U = 10$ ms^{-1}, and $f = 10^{-4}$s^{-1}, boundary layers over land whose depth $h < 1$ km, or boundary layers over the ocean whose depth $h < 0.1$ km, are in the 'weakening' regime.

4 Conclusion

The present study discusses the effect of boundary-layer turbulence on the magnitude of the large-scale vertical velocity. In particular, we confine our analysis to steady-state conditions for low Rossby number flow and we use a bulk, linearized parameterization for the momentum flux. We present new diagnostic relations for the large-scale divergence of horizontal wind (D) and the large-scale vertical velocity, W.

A maximum value for the large-scale divergence D is found if the non-dimensional friction factor k_f is equal to unity, a value which corresponds to a situation in which the actual wind has a cross-isobaric angle of 45°. The factor k_f can be thought of as an Ekman number that weighs the relative importance of the turbulent momentum flux relative to the force due to planetary rotation.

It is argued that the strength of Ekman pumping has a maximum value which can be explained from the following notion. For a purely frictionless geostrophic flow the large-scale divergence of horizontal wind $D = 0$ and consequently there will be no Ekman pumping. The presence of boundary-layer turbulence act as a drag on the flow that generates an ageostrophic flow component giving $D \neq 0$, which, in turn, drives a small large-scale velocity. However, in the limit of infinite turbulent friction the horizontal wind will tend to zero, and likewise $D = 0$. This notion suggests a maximum effect of turbulent friction on the magnitude of D, which is quantified in this study. More precisely, D is found to depend on the curl of the geostrophic wind, or equivalently on the Laplacian of the pressure field, in addition to function F that depends on the non-dimensional friction factor k_{f}.

The findings might be useful to finetune boundary-layer parameterizations and to interpret their effects on the evolution of synoptic-scale systems such as explored in the study by *Sandu et al.* [2013].

References

Beare, R. J. (2007), Boundary layer mechanisms in extratropical cyclones, *Q J R Meteorol Soc*, *133*(623), 503–515.

Bony, S., and B. Stevens (2019), Measuring area-averaged vertical motions with dropsondes, *J Atmos Sci*, *76*(3), 767–783.

Bony, S., B. Stevens, F. Ament, S. Bigorre, P. Chazette, S. Crewell, J. Delanoë, K. Emanuel, D. Farrell, C. Flamant, S. Gross, L. Hirsch, J. Karstensen, B. Mayer, L. Nuijens, J. H. Ruppert, I. Sandu, P. Siebesma, S. Speich, F. Szczap, J. Totems, R. Vogel, M. Wendisch, and M. Wirth (2017), EUREC4A: A field campaign to elucidate the couplings between clouds, convection and circulation, *Surveys in Geophysics*, *38*(6), 1529–1568, doi:10.1007/s10712-017-9428-0.

Ciesielski, P. E., W. H. Schubert, and R. H. Johnson (1999), Large-scale heat and moisture budgets over the ASTEX region, *J Atmos Sci*, *56*(18), 3241–3261.

Edson, J. B., V. Jampana, R. A. Weller, S. P. Bigorre, A. J. Plueddemann, C. W. Fairall, S. D. Miller, L. Mahrt, D. Vickers, and H. Hersbach (2013), On the exchange of momentum over the open ocean, *J Phys Oceanogr*, *43*(8), 1589–1610.

Garratt, J. (1977), Review of drag coefficients over oceans and continents, *Monthly weather review*, *105*(7), 915–929.

Lenschow, D. H., V. Savic-Jovcic, and B. Stevens (2007), Divergence and vorticity from aircraft air motion measurements, *J Atmos Ocean Technol*, *24*(12), 2062–2072.

Lilly, D. (1968), Models of cloud-topped mixed layers under a strong inversion, *Q J R Meteorol Soc*, *94*, 292?–309.

Marshall, J., and R. A. Plumb (2016), *Atmosphere, ocean and climate dynamics: An introductory text*, vol. 21, Academic Press.

Sandu, I., A. Beljaars, P. Bechtold, T. Mauritsen, and G. Balsamo (2013), Why is it so difficult to represent stably stratified conditions in numerical weather prediction (NWP) models?, *J Adv Model Earth Syst*, *5*(2), 117–133.

Schröter, J. S., A. F. Moene, and A. A. Holtslag (2013), Convective boundary layer wind dynamics and inertial oscillations: the influence of surface stress, *Q J R Meteorol Soc*, *139*(676), 1694–1711.

Seibert, P., F. Beyrich, S.-E. Gryning, S. Joffre, A. Rasmussen, and P. Tercier (2000), Review and intercomparison of operational methods for the determination of the mixing height, *Atmos Environ*, *34*(7), 1001–1027.

Seidel, D. J., C. O. Ao, and K. Li (2010), Estimating climatological planetary boundary layer heights from radiosonde observations: Comparison of methods and uncertainty analysis, *J Geophys Res Atmos*, *115*(D16).

Seidel, D. J., Y. Zhang, A. Beljaars, J.-C. Golaz, A. R. Jacobson, and B. Medeiros (2012), Climatology of the planetary boundary layer over the continental United States and Europe, *Journal of Geophysical Research: Atmospheres*, *117*(D17).

Stevens, B. (2006), Bulk boundary-layer concepts for simplified models of tropical dynamics, *Theor. Comput. Fluid. Dyn.*, doi:DOI10.1007/s00162-006-0032-z.

Svensson, G., and A. A. Holtslag (2009), Analysis of model results for the turning of the wind and related momentum fluxes in the stable boundary layer, *Boundary-Layer Meteorol*, *132*(2), 261–277.

Tan, Z.-M. (2001), An approximate analytical solution for the baroclinic and variable eddy diffusivity semi-geostrophic Ekman boundary layer, *Boundary-Layer Meteorol*, *98*(3), 361–385.

Van der Dussen, J. J., S. R. de Roode, and A. P. Siebesma (2016), How large-scale subsidence affects stratocumulus transitions, *Atmos. Chem. Phys.*, *16*, 691–701.

von Engeln, A., and J. Teixeira (2013), A planetary boundary layer height climatology derived from ECMWF reanalysis data, *J Clim*, *26*(17), 6575–6590.

Wu, R., and W. Blumen (1982), An analysis of Ekman boundary layer dynamics incorporating the geostrophic momentum approximation, *J Atmos Sci*, *39*(8), 1774–1782.

Young, G., P. J. Connolly, C. Dearden, and T. W. Choularton (2018), Relating large-scale subsidence to convection development in Arctic mixed-phase marine stratocumulus, *Atmos Chem Phys.*, *18*, 1475–1494.

Zhang, Y., B. Stevens, B. Medeiros, and M. Ghil (2009), Low-cloud fraction, lower-tropospheric stability, and large-scale divergence, *J Clim*, *22*(18), 4827–4844.

Figure.

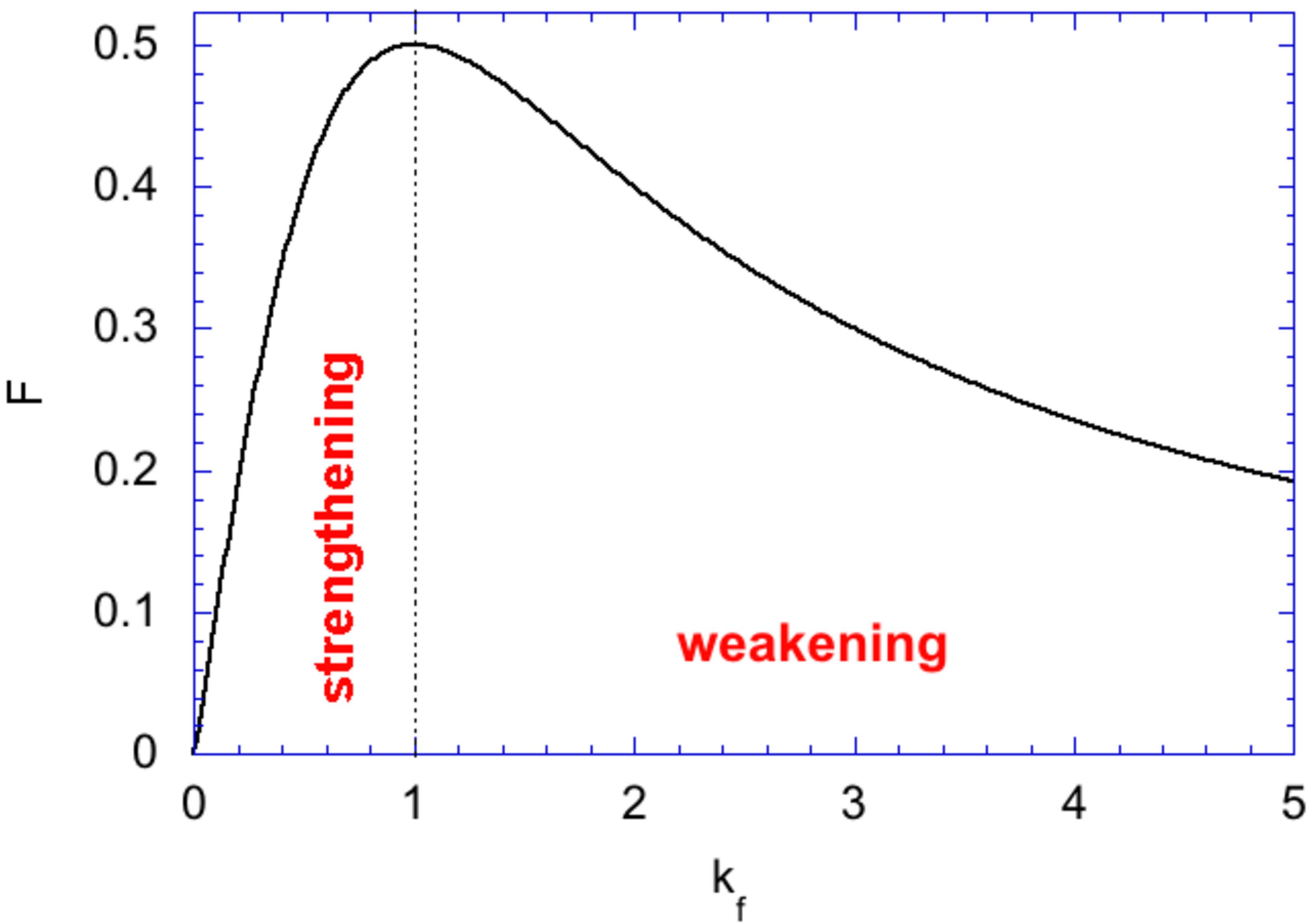

0.5
0.4
0.3
0.2
0.1
0
F
0
1
2
3
4
5
k_f
strengthening
weakening

Figure.

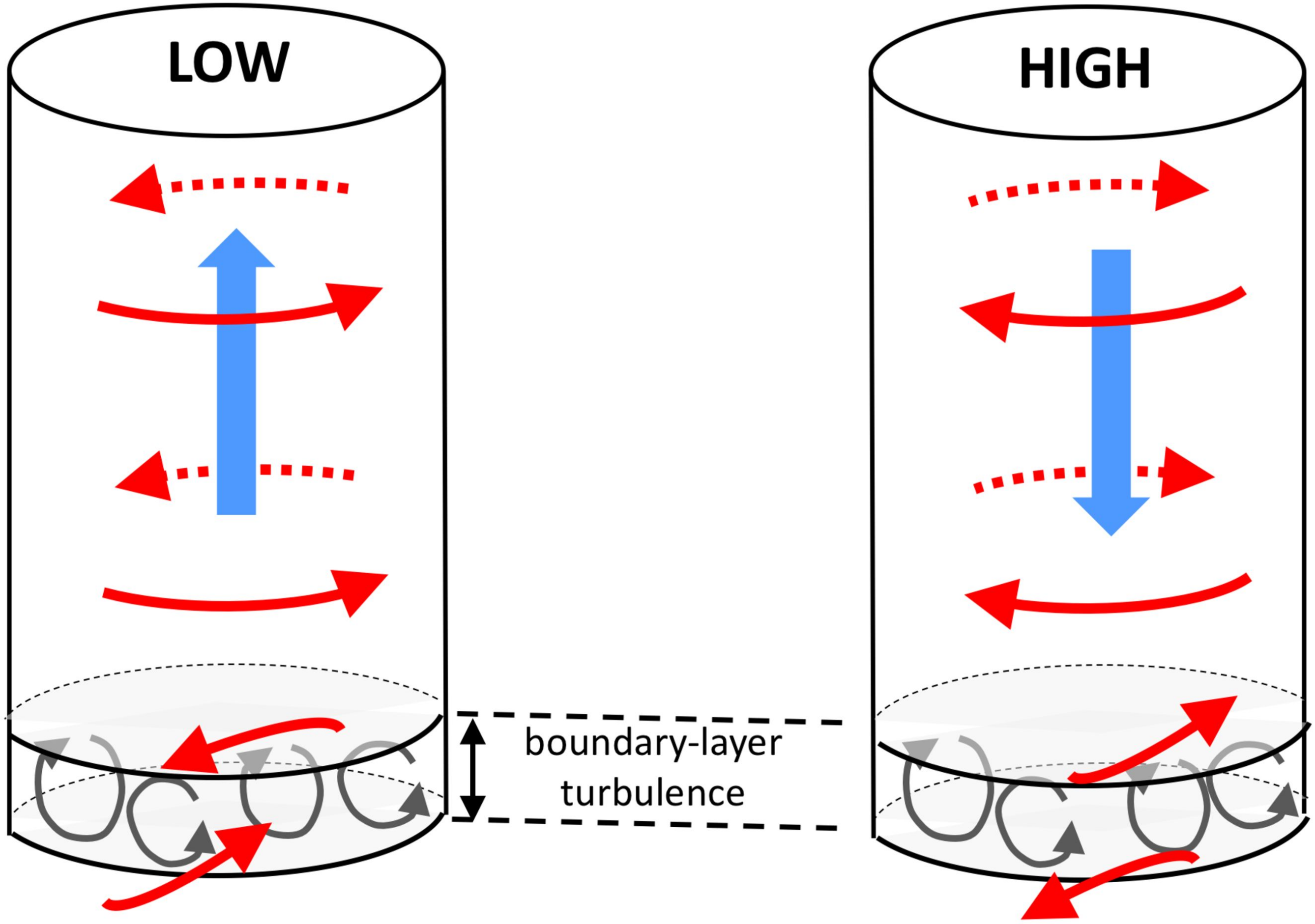
LOW
HIGH
boundary-layer
turbulence